

# EXPERIMENTAL RESULTS FROM THE SMALL ISOCHRONOUS RING \*

E. Pozdeyev, JLab, Newport News, VA 23606, USA  
 F. Marti, R. C. York, MSU, East Lansing, MI 48824-1321, USA  
 J. Rodriguez, CERN, Geneva, Switzerland

## Abstract

The Small Isochronous Ring (SIR) is a compact, low-energy storage ring designed to investigate the beam dynamics of high-intensity isochronous cyclotrons and synchrotrons at the transition energy. The ring was developed at Michigan State University (MSU) and has been operational since December 2003. It stores 20 keV hydrogen beams with a peak current of 10-20 microamps for up to 200 turns. The transverse and longitudinal profiles of extracted bunches are measured with an accuracy of approximately 1 mm. The high accuracy of the measurements makes the experimental data attractive for validation of multi-particle space charge codes. The results obtained in the ring show a fast growth of the energy spread induced by the space charge forces. The energy spread growth is accompanied by a breakup of the beam bunches into separated clusters that are involved in the vortex motion specific to the isochronous regime. The experimental results presented in the paper show a remarkable agreement with simulations performed with the code CYCO. In this paper, we discuss specifics of space charge effects in the isochronous regime, present results of experiments in SIR, and conduct a detailed comparison of the experimental data with results of simulations.

## INTRODUCTION

In recent years, there has been an increased interest in space charge effects in isochronous cyclotrons. Encouraged by the successful high-current operation of the Ring Cyclotron at PSI [1], several authors have proposed an isochronous cyclotron as a driver for a number of applications including radioactive waste transmutation, energy production with accelerator driven nuclear reactors, and generation of neutrons and other secondary particles (see, for example [2]). Tentative designs of such a machine have a maximum beam energy of 1 GeV and a beam current of 10 mA, yielding a total beam power of 10 MW.

Successful operation of a 10 MW cyclotron requires deep understanding of space charge effects in the isochronous regime. Obtaining accurate experimental data on the effect of space charge in large-scale machines is difficult because of resolution and power limitations imposed by diagnostics. Programmatic demands of operating facilities also present a significant complication.

SIR [3],[4] is a compact low-energy storage ring designed to study the dynamics of beams in high-intensity isochronous cyclotrons and synchrotrons at the transition gamma. The ring provides a unique opportunity to perform precise experiments on the effects of space charge. The two main objectives of the ring are the experimental study of space charge effects in the isochronous regime and the validation of multi-particle codes used for space charge simulations.

## SPACE CHARGE EFFECTS IN THE ISOCHRONOUS REGIME

### *Incoherent Transverse Space Charge Effects*

The transverse space charge force decreases the transverse net focusing and lowers the betatron tunes. This effect is dominant in the central region of cyclotrons, where beam energy is low and vertical focusing can be weak. The intensity limit is reached when the vertical size of the beam reaches the vertical aperture limit.

### *Coherent Longitudinal-Radial Vortex Motion*

The energy-phase motion of particles within the beam vanishes in the isochronous regime. This leads to a fast growth of the energy spread within beam bunches. This effect was first mentioned by T. Welton in [5] and later studied in detail by M. Gordon [6], W. Joho [7], and S. Adam [8]. As shown by M. Gordon, space charge forces induce a vortex motion in the beam. The longitudinal component of the space charge force increases/decreases the energy of head/tail particles. The energy-radius coupling causes the particles with deviated energy to move radially. The rate of particle radius change can be expressed as

$$\frac{dx}{d\theta} = \eta \frac{dp/p}{d\theta} \quad (1)$$

where  $\theta$  is generalized azimuthal angle. In the non-relativistic limit, the average value of the dispersion function in the isochronous regime is approximately equal to the average radius of the trajectory,  $R$ . Using expressions for the momentum  $p = mR\omega$  and for the rate of momentum change  $\dot{p} = qE_{||}$ , we rewrite (1) as

$$\frac{dx}{d\theta} = \frac{qE_{||}}{m\omega^2} \quad (2)$$

The longitudinal component of the space charge field is proportional to the total charge of the bunch,  $Q$ :

$$E_{||} = g_{||}Q \quad (3)$$

\* Work supported by NSF Grant #PHY-0110253 and DOE Contract DE-AC05-84ER40150

The geometrical factor  $g_{||}$  includes the dependence on the bunch shape, bunch charge distribution, and particle position within the bunch. Using (3), we obtain the rate of radius change due to energy deviation induced by the space charge force

$$\frac{dx}{d\theta} = g_{||} \frac{qQ}{m\omega^2} \quad (4)$$

A trajectory of a particle with deviated energy is shifted radially relatively to the center of the bunch. A particle offset radially experiences a non-zero average radial space charge force. The radial component of the space charge force changes the radius of the equilibrium trajectory. To calculate an average displacement of the trajectory due to the transverse force we use the equation of particle oscillations with the focusing force substituted by its average value over a turn:

$$\ddot{x} + \nu^2 \omega^2 x = \frac{qE_{\perp}}{m} \quad (5)$$

The steady state solution of this equation is

$$x = \frac{qE_{\perp}}{\nu^2 m \omega^2} \quad (6)$$

As before, we express the transverse electric field through the total charge of a bunch

$$E_{\perp} = g_{\perp} Q \quad (7)$$

where the geometrical factor  $g_{\perp}$  depends on the beam shape, bunch charge distribution, and radius of equilibrium orbit relative to the center of the bunch. Replacing  $E_{\perp}$  from (7) into (6) yields

$$x = g_{\perp} \frac{qQ}{\nu^2 m \omega^2} \quad (8)$$

The transverse component of the space charge force shifts the particle off the equilibrium orbit but does not change the particle energy and velocity. This causes the particle to slip in phase. The separation between a particle on the equilibrium orbit and a particle on the shifted orbit grows as

$$ds = -x d\theta \quad (9)$$

This yields the rate of longitudinal slip under the transverse space charge force

$$\frac{ds}{d\theta} = -g_{\perp} \frac{qQ}{\nu^2 m \omega^2} \quad (10)$$

In isochronous cyclotrons, the radial betatron tune is approximately equal to the relativistic factor  $\gamma$ , which is, in turn, equal to 1 in the low-energy limit. Thus, the particle slips with a rate given by

$$\frac{ds}{d\theta} \approx -g_{\perp} \frac{qQ}{m\omega^2} \quad (11)$$

From (4) and (11), one can see, the vortex motion depends on the beam shape, particle position within a bunch, and the ratio

$$\frac{qQ}{m\omega^2} \quad (12)$$

Thus, two bunches similar in shape in two different cyclotrons behave alike (per turn) if expression 12 yields the same value for both bunches.

## CHOICE OF BEAM PARAMETERS FOR SIR

SIR is designed to run low energy light-ion beams. This choice of beam parameters simplifies the ring design and minimizes the cost of the project. The low beam energy yields a low velocity of ions. Because space charge effects scale as  $I_{\text{peak}}/(\gamma\beta)^3$ , only low intensity beam is required to reach the interesting space charge regime. The low particle velocity also relaxes the timing requirements on the diagnostics and on the injection-extraction system. The low beam energy allows the use of simple, low-field magnetic elements.

The University of Maryland Electron Ring (UMER) group [9] uses a low energy electron beam to study space charge effects. Both rings SIR and UMER are designed for approximately the same beam energy range: tens of keV. However, the  $\text{H}_2^+$  beam in SIR is approximately 40 times slower than the electron beam of in UMER. This allows us to use less expensive diagnostics to measure the longitudinal beam distribution. The magnetic rigidity of the ion beam is approximately 90 times higher than that of the electron beam. This makes the ion beam significantly less sensitive to stray magnetic fields and eliminates the problem of the earth magnetic field.

Table 1: The generalized perviance normalized on the beam current, the magnetic field of a 45-cm-radius bend, and the particle velocity of low energy light ion and electron beams.

	$\text{H}_2^+, \text{D}$ (20 keV)	Electrons (10 keV)
$K/I_{\text{peak}}$	3.2e-1	1.6e-2
$B_{\rho=0.45m}$ (Gauss)	640	7.5
$\beta$	4.6e-3	0.2

## SIR DESIGN

SIR consists of four 90°, flat-field magnets with edge focusing. The edge focusing provides both the vertical focusing and the isochronism in the ring. Figure 1 shows a photograph of SIR. Table 2 gives the primary ring parameters. An  $\text{H}_2^+$  beam is produced by a multi-cusp ion source, that can be biased up to 30 kV. An analyzing magnet located under the ion source provides charge-to-mass state selection and steers the beam towards the ring. In the injection line, the selected beam is chopped by a chopper and matched to the ring by a triplet of electrostatic quadrupoles. The bunch length can be changed from 100 nanoseconds to 4 microseconds. The beam is injected into the ring by a fast pulsed electrostatic inflector. After injection, the bunch

coasts in the ring. After a chosen number of turns, the bunch is deflected towards either a phosphor screen or a Fast Faraday Cup (FFC) situated above and below the median plane respectively. The Faraday Cup measures the longitudinal beam profile of the beam with a time resolution of 1 ns corresponding to a spatial resolution of 1.5-2 mm. The phosphor screen is used to register the transverse beam profile. Using this procedure, we can take "snapshots" of the longitudinal and radial beam profiles after a different number of turns.



Figure 1: Small Isochronous Ring

Table 2: Primary SIR parameters.

Beams	$H_2^+$
Energy	5-30 keV
$\nu_x, \nu_y$	1.14, 1.11
$\alpha_p - 1/\gamma^2$	$< 3e - 3$
Bend radius	0.45 m
Bend field	800 Gauss
Rev. period	5 $\mu$ sec
C	6.6 m
$N_{\text{turns}}$	100
$I_{\text{peak}}$	0-25 $\mu$ A

## SIMULATIONS OF THE BEAM DYNAMICS IN SIR

Two computer codes have been used to calculate the beam dynamics in SIR: CYCO [10] and Warp3D [11]. Both codes predicted quite well the observed behavior. Most of the simulations were performed with CYCO.

Figure 2 shows an example of the simulated beam dynamics in SIR for three peak beam current values: 5, 10, and 20  $\mu$ A. The longitudinal space charge force increases the energy of the head particles and decreases the energy of the tail particles. Due to the isochronous condition the head moves toward larger radii and the tail toward smaller radii. After a few turns, the bunch breaks up into small clusters. The breakup happens almost simultaneously everywhere throughout the bunch.

The charge density of the bunch has to be integrated in the transverse dimensions to simulate a response of the Faraday Cup. Figure 3 shows the linear charge density of the bunch distributions shown in Figure 2.

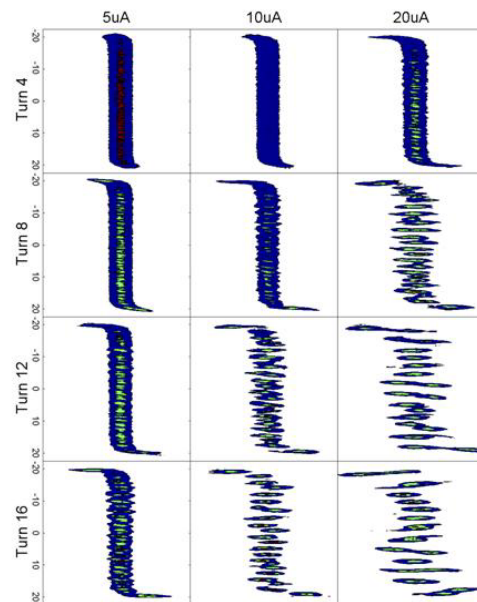


Figure 2: Results of simulations of the beam dynamics in SIR calculated with CYCO. The figure shows the charge density contour plots for three values of the beam current and for four turns. The energy of the  $H_2^+$  beam is 20 keV.

## EXPERIMENTAL STUDIES OF THE BEAM DYNAMICS IN SIR

### SIR Optics Characterization

The beam injected off-axis oscillates in the ring around the closed orbit. Because of these oscillations the displacement of the extracted beam on the phosphor screen depends on turn number. Fitting the precession of the beam spot on the phosphor screen to a sine function, we obtained the betatron tunes of the beam. The measured horizontal and vertical betatron tunes,  $\nu_x$  and  $\nu_y$ , were 1.142 and 1.110 respectively. Note that the designed values of the betatron tunes, calculated from simulations of the beam dynamics in SIR, were 1.143 and 1.128 for  $\nu_x$  and  $\nu_y$  respectively.

The ring isochronism was measured by the time-of-flight technique. The beam energy was changed by  $\pm 1\%$  from its equilibrium value and corresponding change of the arrival time to the Faraday Cup after 200 turns was recorded. The measured slip factor,  $\alpha - 1/\gamma^2$ , was smaller than  $3 \cdot 10^{-3}$ .

### Beam Life-Time

Figure 4 shows the beam current in SIR vs. turn number for different values of the residual gas pressure in the ring.

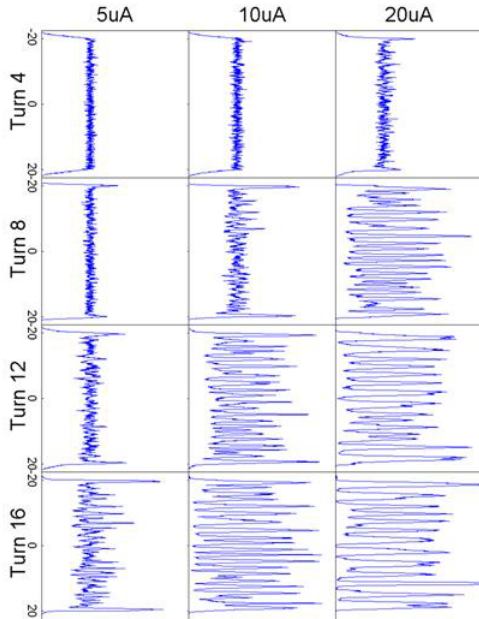


Figure 3: Simulated response of the Faraday Cup obtained by integration of the beam profiles shown in Figure 2 in the transverse dimensions.

The beam energy was 21 keV. Fitting the curves with the function

$$I = I_0 \exp(-n/N), \quad (13)$$

we conclude that the life time measured in turns in the ring depends on the average pressure as

$$N = 100 \frac{2 \cdot 10^{-7}}{P(\text{Torr})} \quad (14)$$

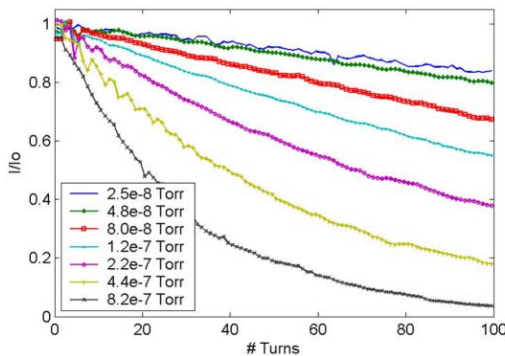


Figure 4: Average current of the  $H_2^+$  beam vs. turn number for different values of the residual gas pressure in the ring. Each curve was normalized on the corresponding maximum current value.

### Transverse Beam Dynamics with Space Charge

Figure 5 shows the beam spot of the extracted 20 keV  $H_2^+$  beam for turns 2 to 16 with an interval of 2 turns. The

bunch peak current was  $20 \mu\text{A}$  and the bunch length was  $1 \mu\text{sec}$ . The fast increase of the bunch width is indicative of a rapid increase of the beam energy spread. The energy spread at turn 16 can be estimated as

$$\frac{\delta E}{E} = 2 \frac{X_{16} - X_2}{\eta} = 5\%, \quad (15)$$

where  $X_i$  is the horizontal beam size at the  $i^{\text{th}}$  turn and  $\eta$  is the dispersion function at the extraction region equal to 932 mm.

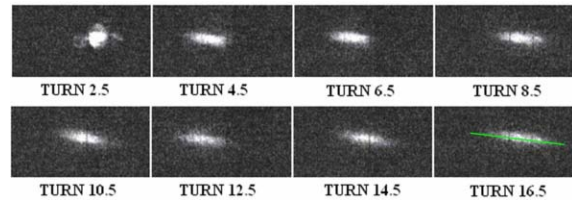


Figure 5: Beam spot produced by the extracted beam on the phosphor screen situated in the extraction region. Each frame is approximately 60 mm by 30 mm. The green line in the last frame is tilted by  $7^\circ$  and is approximately parallel to the beam spot. This supports the presumption that the beam width increases due to the energy spread growth (see the text for detailed discussion).

The obvious tilt of the beam spot supports the presumption of the fast energy spread growth. The dependence of the deflection angle on the particle energy causes particles with different energies to hit the phosphor at different heights. Particles with different energies also displaced horizontally according to  $x = \eta \cdot \delta p/p$ . The correlation between the vertical and horizontal displacements manifests itself as a tilt of the spot of the extracted beam. The tangent of the tilt angle is

$$\tan(\theta) = -2 \frac{y_0}{\eta}, \quad (16)$$

where  $y_0$  is the average vertical displacement of the beam spot from the median plane. The measured  $y_0$  is approximately 58 mm, yielding a tilt angle of approximately  $7.1^\circ$ . According to Figure 5, the bunch after 16 turns is tilted at approximately  $7^\circ$ .

### Longitudinal Beam Dynamics with Space Charge

Figure 6 shows the longitudinal profile of beam bunches extracted after turns 4, 8, 12, and 16 for three different values of the beam current: 5, 10, and  $20 \mu\text{A}$ . The beam profiles were measured by the Faraday Cup and recorded by a digital oscilloscope.

A comparison of the experimental data and the simulations results can be done by counting the number of clusters for each turn. Figure 7 shows the number of clusters for different peak currents as a function of turn number for 5, 10, and  $20 \mu\text{A}$ . The figure also represents the standard deviation of the distribution of 100 measurements.

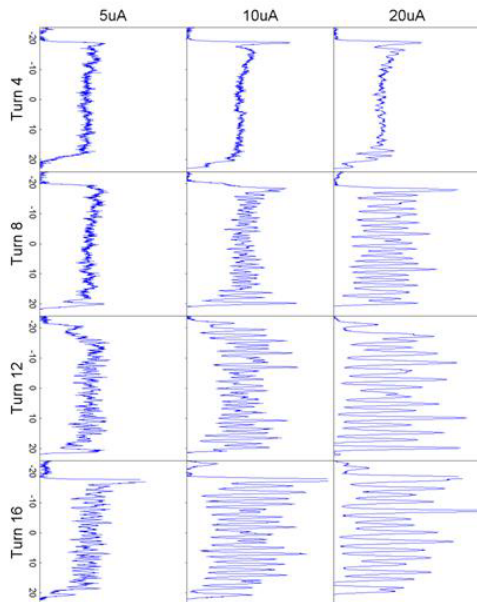


Figure 6: Longitudinal beam profile of the 20 keV  $H_2^+$  measured by the Faraday Cup for three different beam currents and four different turns.

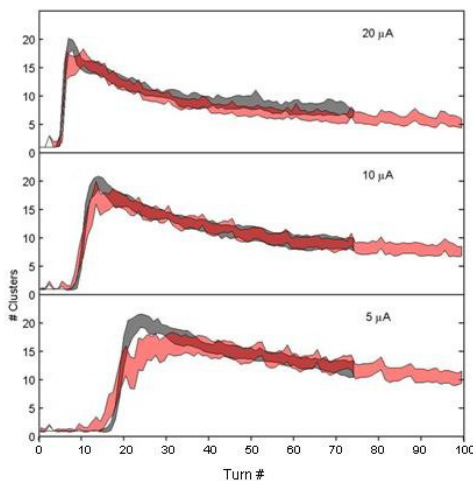


Figure 7: The number of clusters in a beam bunch vs. turn number for three different beam currents measured by the Faraday Cup (red) and simulated by CYCO (gray). The curves are obtained by averaging over 100 measurements. The width of the curves shows the standard deviation of the distribution of the 100 samples.

## CONCLUSIONS

The small isochronous ring has been developed and successfully operated at the National Superconducting Cyclotron Lab at Michigan State University. Operational experience with SIR has shown that the ring is reliable and easy to operate. The primary ring parameters including the betatron frequencies, isochronism, and the beam life-time

are close to designed values.

Experimental beam dynamics studies at SIR showed that the space charge force induces a fast growth of the energy spread within a bunch accompanied by a longitudinal breakup of the bunch. The experimental results show a remarkable agreement with simulation results obtained with multi-particle codes CYCO and Warp3D.

## ACKNOWLEDGEMENT

We would like to thank D. Devereaux, R. Fontus, D. Sanderson, A. Zeller and R. Zink of NSCL for extensive help during the design and construction of SIR. We would also like to thank Lawrence Berkeley National Laboratory for lending us the multi-cusp source used in SIR and to D. P. Grote from LBNL for help in setting up Warp3D.

## REFERENCES

- [1] T. Stambach et al., "The PSI 2 mA Beam and Future Applications", Proc. of Cyclotrons 2001, p. 423 (East Lansing)
- [2] Th. Stambach et al., "The 0.9 MW Proton Beam at PSI and Studies on a 10 MW Cyclotron", Proc. 2nd Int. Conf. on Accelerator-Driven Transmutation Technologies, Kalmar 1996, p.1013
- [3] E. Pozdeyev et al., "Progress Report on the Small Isochronous Ring Project at NSCL", Proc. of PAC 2003, p. 138 (Portland)
- [4] J.A. Rodriguez, F. Marti, E. Pozdeyev, and R.C. York, "Experimental Results of the Small Isochronous Ring", Proc. of EPAC 2004, p. 2194 ( Lucerne)
- [5] T. Welton, "Sector focused Cyclotrons", Nucl. Sci. Ser. Report No. 26, NAS-NRC-656, (192, Washington D.C., 1959)
- [6] M.Gordon, 5th Int. Cycl. Conf. (Oxford, 1969), p.305, Butterworth, London.
- [7] W.Joho, 9th Int. Cycl. Conf. (Caen, 1981), p.337, Les editions de physique, Les Ulis Sedex.
- [8] S.Adam, 14th Int. Cycl. Conf. (Cape Town, 1995), p.446, World Scientific, Singapore.
- [9] P. O'Shea et al., "The University of Maryland Electron Ring," Procs. of PAC2001 (Chicago), p. 159
- [10] E. Pozdeyev, Ph.D. dissertation, MSU, 2003.
- [11] D. P. Grote, A. Friedman, I. Haber, "Methods used in WARP3d, a Three-Dimensional PIC/Accelerator Code", Proc. of the 1996 Comp. Accel. Physics Conf., AIP Conference Proceedings 391, p. 51 (1996).